EUROPEAN ORGANIZATION FOR NUCLEAR RESEARCH

CERN-PPE/95-xx

SEARCH FOR A NEW LIGHT GAUGE BOSON IN DECAYS OF π^0, η AND η'

C. Amsler[15], D.S. Armstrong[1,a], C.A. Baker[5], B.M. Barnett[11], C.J. Batty[5], M. Benayoun[6], K. Beuchert[2], P. Birien[1], P. Blüm[8], R. Bossingham[1], K. Braune[12], J. Brose[11], D.V. Bugg[9], T. Case[1], A. Cooper[9], O. Cramer[12], K.M. Crowe[1], T. Degener[2], H.P. Dietz[12], N. Djaoshvili[6], S. v. Dombrowski[15], M. Doser[6], W. Dünnweber[12], D. Engelhardt[8], M. Englert[12], M.A. Faessler[12], C. Felix[12], T. Gemesy[4], P. Giarritta[15], R. Hackmann[11], R.P. Haddock[10], F.H. Heinsius[1], M. Herz[2], N.P. Hessey[12], P. Hidas[4], P. Illinger[12], D. Jamnik[12,d], H. Kalinowsky[11], B. Kämmle[7], T. Kiel[8], J. Kisiel[6,e], E. Klempt[3], M. Kobel[6,f], H. Koch[2], C. Kolo[12], M. Kunze[2], M. Lakata[1], R. Landua[6], J. Lüdemann[2], H. Matthäy[2], R. McCrady[13], J.P. Merlo[11], C.A. Meyer[13], L. Montanet[6], A. Noble[15,i], R. Ouared[6], F. Ould-Saada[15], K. Peters[2], C.N. Pinder[5], S. Ravndal[2,h], C. Regenfus[12], E. Schäfer[11], P. Schmidt[7], R. Seibert[7], S. Spanier[11,j], H. Stöck[2], C. Straßburger[3], U. Strohbusch[7], M. Suffert[14], U. Thoma[3], M. Tischhäuser[8], D. Urner[15], C. Völcker[12], F. Walter[11], D. Walther[2], U. Wiedner[7], N. Winter[8], J. Zoll[6], B. Zou[9], Č. Zupančič[12]

The Crystal Barrel Collaboration

to be submitted to Phys. Rev. or Nucl. Phys.

1) University of California, LBL, Berkeley, CA 94720, USA
2) Universität Bochum, D-44780 Bochum, Germany
3) Universität Bonn, D-53115 Bonn, Germany
4) Academy of Science, H-1525 Budapest, Hungary
5) Rutherford Appleton Laboratory, Chilton, Didcot OX11 0QX, UK
6) CERN, CH-1211 Genève, Switzerland
7) Universität Hamburg, D-22761 Hamburg, Germany
8) Universität Karlsruhe, D-76021 Karlsruhe, Germany
9) Queen Mary and Westfield College, London E1 4NS, UK
10) University of California, Los Angeles, CA 90024, USA
11) Universität Mainz, D-55099 Mainz, Germany
12) Universität München, D-80333 München, Germany
13) Carnegie Mellon University, Pittsburgh, PA 15213, USA
14) Centre de Recherches Nucléaires, F-67037 Strasbourg, France
15) Universität Zürich, CH-8057 Zürich, Switzerland
a) Now at William & Mary College, Williamsburg, VA 23187, USA
b) Now at Universität Siegen, Siegen, Germany
c) Now at University of Kent, Canterbury, UK

d) On leave of absence from the University of Ljubljana, Ljubljana, Slovenia
e) On leave of absence from the University of Silesia, Katowice, Poland
f) Now at Universität Freiburg, Freiburg, Germany
g) Now at Max-Planck-Institut, Heidelberg, Germany
h) Now at CERN, Genève, Switzerland
i) Now at CRPP, Ottawa, Canada
j) Now at Universität Zürich, Zürich, Switzerland

Abstract

Upper limits for the production of new light gauge bosons in π^0, η and η' decays have been obtained with the Crystal Barrel detector. The kinematically well-constrained reactions $\overline{p}p \rightarrow \pi^0\pi^0 P$ have been studied, where $P \equiv \pi^0, \eta, \eta'$ decays through the emission of a single photon recoiling against a missing state X. X can be a long-lived weakly interacting particle or $X \rightarrow \nu\overline{\nu}$. This paper gives full detail of the analysis of our previous work and extends the search to η' decay. No signal has been observed and branching ratio upper limits (90 % $C.L.$) of 6×10^{-5} have been obtained for masses of the gauge boson lying between $\sim$ 65 MeV and 125 MeV (π^0 decay), 6×10^{-5}, for X masses between $\sim$ 200 MeV and 525 MeV (η decay), and 4×10^{-5}, for X masses between $\sim$ 50 MeV and 925 MeV (η' decay). The π^0-decay limit represents a factor of 4 to 8 (depending on the X-mass) improvement when compared to the existing limit, whereas the η and η' decay limits have been measured for the first time, thereby extending the M_X range from 125 MeV up to 925 MeV.

1 Introduction

Various extensions of the Standard Model (SM) of strong and electroweak interactions, $SU(3) \times SU(2)_L \times U(1)$ exist. Some of them require an extra gauge group $U'(1)$ and, hence, a new gauge boson X. This possibility is realised in grand unified theories [1], in supersymmetric theories [2], in superstring-inspired models [3] and in models including a new long-range interaction, the fifth force [4]. Another alternative to the SM has been considered in [5], based on the richer group $SU(3)_L \times SU(3)_R \times SU(2)_L \times U(1)$. A massive color octet of gauge bosons, the axigluon, has been introduced. Some X bosons could be light enough to be detected in rare or (SM) forbidden decays of light mesons (π,K,η,..) [6, 7]. To look for such new light particles, with masses of the order of the pion mass and with small couplings, high rates and precision are needed. Constraints on branching ratios for the decay of a pseudoscalar[1]

$$P \rightarrow \gamma X \tag{1}$$

P being a π^0, an η or an η' are given in reference [7]. They range from 10^{-7} to 10^{-3} and are based on earlier measurements in the case of π^0 and on models for η and η'. Before the data from the Crystal Barrel experiment [8] were available, only measurements of $\pi^0 \rightarrow \gamma X$ had been performed. The best upper limit of 4×10^{-6} ($40 < M_X < 100$ MeV/c^2) has been obtained for the special decay mode $X \rightarrow e^+e^-$ [9]. The results from $\pi^0 \rightarrow \nu\overline{\nu}$ [10] have been interpreted as giving a limit of 6.2×10^{-6} on $BR(\pi^0 \rightarrow \gamma\nu\overline{\nu})$ [7]. This, however, is not a direct measurement. Branching ratio upper limits for the π^0 decay have been published by two other experiments at BNL and TRIUMF 5×10^{-4} [11] and $(2-7) \times 10^{-3}$ [12], respectively, for the case $X \rightarrow$ "anything". Throughout the whole paper "anything" includes $X \rightarrow e^+e^-, \nu\overline{\nu}$ and $X \rightarrow \mu^+\mu^-$ (for η, η'), and the case where X has a long lifetime and does not decay in the detector.

In reference [8] we have already published results concerning the decays

$$\pi^0 \rightarrow \gamma X \tag{2}$$

$$\eta \rightarrow \gamma X, \tag{3}$$

where $X \rightarrow$ "unseen" (X does not decay nor interact in the detector or $X \rightarrow \nu\overline{\nu}$). The decays $X \rightarrow e^+e^-, \mu^+\mu^-$ are not considered.

In this work we give more information about the analysis and extend the search for the X boson to the decay

$$\eta' \rightarrow \gamma X. \tag{4}$$

The results have been first presented in reference [13].

2 Signature

Consider the decay $P \rightarrow \gamma\gamma$. In the rest frame of the decaying pseudoscalar P, the photon energy is given by $E^*_\gamma = m_P/2$, where m_P is the mass of the pseudoscalar P. Because

[1]The advantage of $P \rightarrow \gamma X$ over $K^+ \rightarrow \pi^+ X$ is the unambiguous theoretical interpretation: if there is a signal it can only be a spin-1 (gauge) boson [6]. We will see that our search includes any vector bosons with similar properties.

of detector inefficiencies, one of the two photons can be lost. This leads to a peak at $E_\gamma^* = m_P/2$ in the energy distribution with a width determined by the experimental resolution. If one replaces the missing photon by a missing massive gauge boson X, the photon energy distribution peaks at

$$E_\gamma^* = \frac{m_P}{2}\,(1 - \frac{M_X^2}{m_P^2}), \tag{5}$$

where M_X is the mass of the gauge boson X. Fig.1 shows the dependence of M_X on E_γ^*. To look for a hypothetical gauge boson X in the decays $P \to \gamma X$ we exploit the fact that

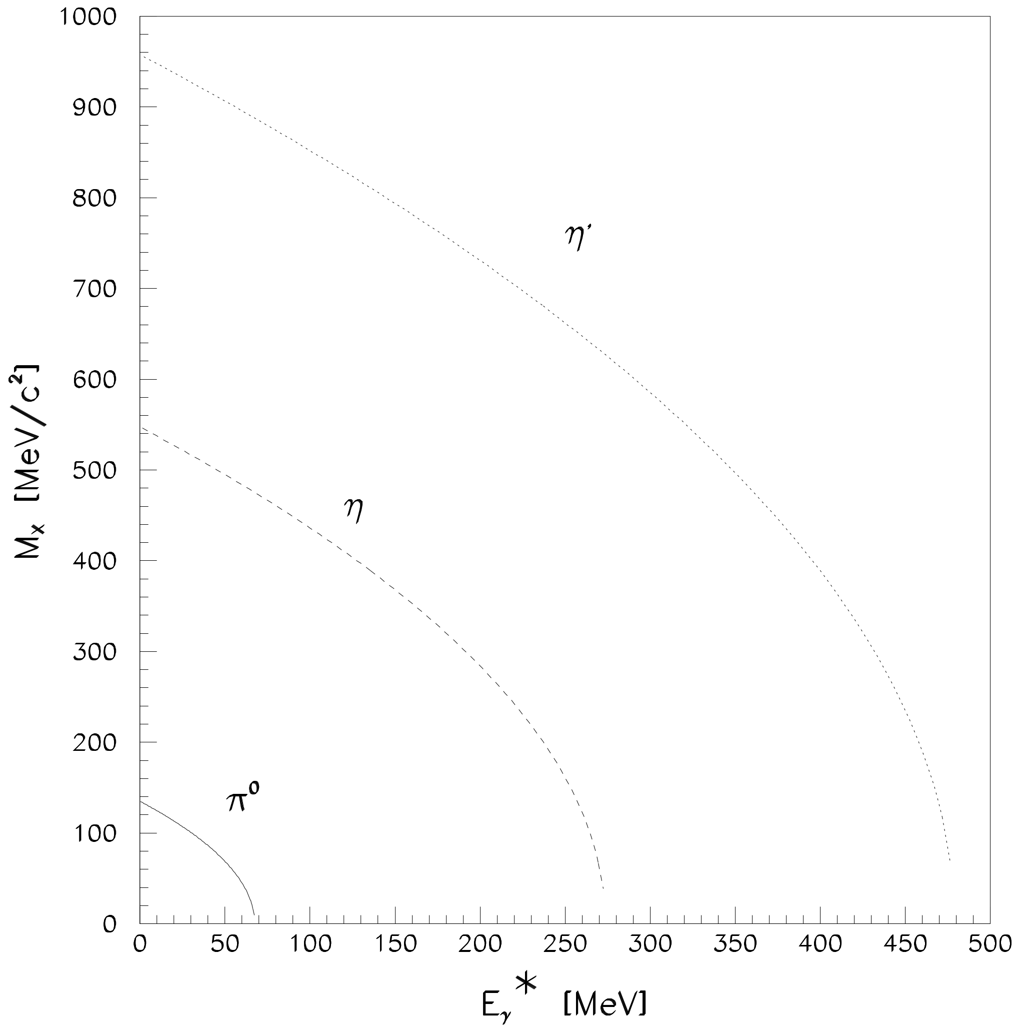

Figure 1: *Decay $P \to \gamma X$: Mass of X as a function of the energy of the photon in the centre of mass of the pseudoscalar $P \equiv \pi^0, \eta, \eta'$.*

the annihilation of antiprotons with protons is a rich source of mesons (e.g., $\pi^0, \eta, \eta', \omega$)

and that the Crystal Barrel detector is ideally designed for measurements of final states with many photons. We use the well-constrained reactions

$$\bar{p}p \to \pi^0\pi^0\pi^0 \tag{6}$$

$$\bar{p}p \to \pi^0\pi^0\eta \tag{7}$$

$$\bar{p}p \to \pi^0\pi^0\eta' \tag{8}$$

because of the relatively high branching ratios $BR(\bar{p}p \to \pi^0\pi^0\pi^0) = (0.62 \pm 0.10)\%$ [14], $BR(\bar{p}p \to \pi^0\pi^0\eta) = (0.65 \pm 0.07)\%$ [15] and $BR(\bar{p}p \to \pi^0\pi^0\eta') = (0.40 \pm 0.08)\%$ (preliminary) [16] at rest in liquid hydrogen.

3 Detector and Data Selection

The data have been collected using the Crystal Barrel detector at the Low Energy Antiproton Ring (LEAR) at CERN. Antiprotons with a momentum of 200 MeV/c are stopped in a 4-cm-long liquid hydrogen target. A matrix of silicon counters in front of the target defines and monitors the incident $\bar{p}$ beam (typically 10^4 $\bar{p}/s$). The target is surrounded by two cylindrical proportional wire chambers (PWCs), a jet drift chamber (JDC) to detect charged particles, and a barrel-shaped calorimeter consisting of 1380 CsI(Tl) crystals, 16 radiation lengths deep, with photodiode readout. The CsI calorimeter covers the polar angles between 12° and 168° with full coverage in azimuth. The useful acceptance for shower detection is $0.95 \times 4\pi$ sr. The energy calibration is provided by $\pi^0 \to 2\gamma$ decays by imposing the mass of the π^0. The energy resolution, which varies slightly from run to run, is given by

$$\frac{\sigma_E}{E_\gamma} \sim \frac{2.5\%}{\sqrt[4]{E_\gamma/\mathrm{GeV}}}. \tag{9}$$

The angular resolution (polar and azimuthal) $\sigma_{\theta,\phi}$ varies with the photon energy from 20 mrad to 35 mrad for isolated showers and is $\sim$ 35 mrad for two or more showers when merged into a single cluster of crystals. The whole assembly is located in a solenoid magnet providing a homogeneous field of 1.5 T parallel to the incident $\bar{p}$ beam. A more detailed description of the detector, the trigger conditions and the reconstruction procedure is given in Ref. [17].

The analysis is based on 15×10^6 (18×10^6 for η') triggered "all-neutral" events. The triggering was performed using the PWCs and the inner layers of the JDC to veto charged tracks. Events with residual charged tracks are removed in the offline data selection. Thus $1,019,634$ ($1,223,567$ for η') events containing exactly 5 electromagnetic showers (PEDs) with energy deposits exceeding the threshold energy $E_{cut} = 20$ MeV are selected. Events with a PED induced in the last crystal rows (crystal type 13) around the beam entrance and exit pipes are removed to suppress energy leakage. Shower fluctuations may produce fake photons, so-called split-offs. These are characterised by their small energy and their proximity to a higher energy PED. Such split-off events are suppressed by requiring the relative energy deposition of two neighbouring PEDs, the centroids of which are separated by less than 14°, to be larger than 0.18. After these cuts $818,655$ events ($982,386$ for η')

are left. The next step is to reconstruct two π^0s out of the 5γ sample. The invariant masses of all combinations of two photons are calculated and events containing two π^0s and a single γ are kept. When more than one combination is found, only the best configuration with a confidence level $C.L. > 2.7\%$ is chosen. The surviving data sample consists of $186,764$ ($197,748$ for η') events. Once the $\pi^0\pi^0\gamma$ events are selected, a kinematic fit with three constraints (3-C fit) ($\pi^0\pi^0 P_{miss}$, where P_{miss} is a missing π^0, a missing η or a missing η') is performed, ignoring the remaining single photon. A confidence level greater than 15% is required. As a result of the fit the momentum of the missing particle P_{miss} is determined and $95,392$ $\pi^0\pi^0\pi^0_{miss}$, $17,943$ $\pi^0\pi^0\eta_{miss}$ and $4,165$ $\pi^0\pi^0\eta'_{miss}$ events survive.

Table 1 gives a summary of the selected and fit events. The method used to search

Cuts	Events (π^0)	Events (η)	Events (η')
0-prong events	15,000,000	15,000,000	18,000,000
5γ, $E_\gamma \geq$ 20 MeV	1,019,639	1,019,639	1,223,567
no crystal type 13	857,456	857,456	1,028,947
no split-offs	818,655	818,655	982,386
$\pi^0\pi^0\gamma$	186,764	186,764	197,748
$\pi^0\pi^0 P_{miss}$ (fit, C.L. $\geq$ 0.15)	95,392	17,943	4,165
$\overline{fit}$ $5\gamma + \gamma_{miss}$ rejection	54,311	10,827	2,848
ω rejection	46,158	-	-
$K_L K_S$ rejection	-	8,961	2,820
$\overline{fit}$ $\pi^0\pi^0 P_{miss}$	36,217	7,324	2,387
$E_\gamma^{lab}/E_\gamma^*$ cut	24,503	5,121	2,198

Table 1: *Data reduction and final data sample.*

for an X signal now consists of plotting the energy E_γ^* of the single γ in the rest frame of P_{miss}. The measured energy and momentum of the fifth photon (which is ignored by the fitting procedure) and the fit values of P_{miss} are used to calculate E_γ^*.

4 Background reduction

The background contribution can be split into two categories: 5γ final states without and with missing energy and momentum We first discuss the cuts used to reduce these two categories (sections 4.1 and 4.2). In a third section we give more details about the remaining background.

4.1 5γ final states without missing energy and momentum

The first source of background comes from real $\pi^0\pi^0\gamma$ events, due to the finite resolution of the detector. Here it is mainly the channel $\bar{p}p \to \omega\pi^0$ ($\omega \to \pi^0\gamma$) which feeds into the fit $\pi^0\pi^0\pi^0_{miss}$ and to a lesser extent into $\pi^0\pi^0\eta_{miss}$. These events are responsible for the ω peak around 780 MeV in the $\pi^0\pi^0_{miss}$ invariant mass distribution (Fig.2). To reduce this background the selected 5γ data events are kinematically fit to the following final states:

- $\bar{p}p \to \pi^0\omega$ ($\omega \to \pi^0\gamma$) (7-C fit),

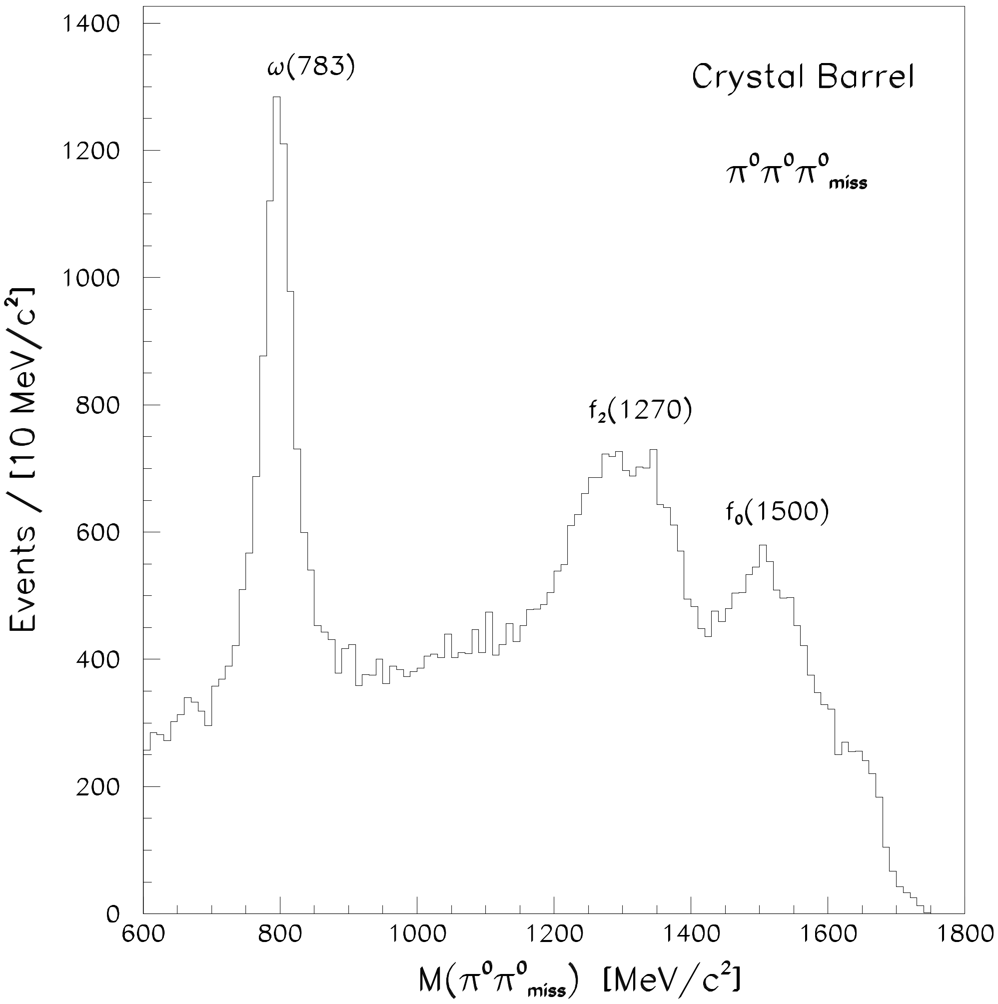

Figure 2: *Fit $\pi^0\pi^0\pi^0_{miss}$ event sample: $\pi^0\pi^0_{miss}$ invariant mass distribution showing the $\omega(783)$, the $f_2(1270)$ and the $f_0(1500)$.*

- $\overline{p}p \to \eta\omega$ ($\omega \to \pi^0\gamma$ and $\eta \to \gamma\gamma$) (7-C fit),

- $\overline{p}p \to \pi^0\eta\gamma$ (6-C fit) and

- $\overline{p}p \to \eta\eta\gamma$ (6-C fit).

If one of the 5γ combinations fits one of the above final states with a $C.L. > 1\%$, the event is rejected ($\overline{fit}$ 5γ in table 1). To improve our $\omega\pi^0$ rejection events are rejected for which the invariant mass $M(\pi^0\gamma)$ is in the region $755 \leq M_{\pi^0\gamma} \leq 805$ MeV/c^2 and the angle between the π^0 direction and the fifth photon is larger than 167°. About 25% of events are rejected for $\pi^0\pi^0\pi^0_{miss}$, while the proportion of rejected events is negligible in the case of $\pi^0\pi^0\eta_{miss}$ and $\pi^0\pi^0\eta'_{miss}$ (ω rejection in table 1).

4.2 5γ final states with missing energy and momentum

The second source of background consists of the following final states: $\overline{p}p \to \pi^0\pi^0\pi^0$, where one photon from a π^0 is undetected and $\overline{p}p \to \pi^0\pi^0\eta$ (η'), where one photon from the η (η') is undetected. In the $\pi^0\pi^0\pi^0_{miss}$ event sample the missing photon background is responsible for two structures in the $\pi^0\pi^0_{miss}$ invariant mass distribution (Fig.2): $f_2(1270) \to \pi^0\pi^0$ and $f_0(1500) \to \pi^0\pi^0$. There are two main ways in which a photon can escape detection. Either the γ is lost around the beam entrance or exit pipes ($\theta \geq 168°$ or $\theta \leq 12°$) or between the two halves of the barrel ($\theta \sim 90°$) or, alternatively, its energy is below the detection threshold of 20 MeV. The polar angular distribution of the missing photon direction is plotted in fig.3. This quantity is deduced from the fit P_{miss} and the measured fifth photon. In order to reduce the missing photon contribution, an event is discarded if $|\cos(\theta_{\gamma_{miss}})| \geq 0.95$ or $|\cos(\theta_{\gamma_{miss}})| \leq 0.02$ (γ_{miss} rejection in table 1).
After the background rejection due to 5γ final states without and with missing energy and momentum, we are left with $46,158$ $\pi^0\pi^0\pi^0_{miss}$, $10,827$ $\pi^0\pi^0\eta_{miss}$ and $2,848$ $\pi^0\pi^0\eta'_{miss}$ events (table 1).

For the η decay we also take into account the channel $\overline{p}p \to K_S K_L$, where $K_S \to \pi^0\pi^0$ and K_L interacts in the barrel and produces one PED. This background is relevant since the mass of K_L (497.67 MeV/c^2) is close to the η mass (547.45 MeV/c^2). The K_L and K_S emerge back to back and therefore events are rejected for which the invariant mass of the two π^0s is in the region[2] $455 \leq M_{\pi^0\pi^0} \leq 506$ MeV/c^2 and for which the angle between the K_S direction and the fifth photon is greater than 167°. The $\pi^0\pi^0$ invariant mass is shown in fig.4 before (full histogram) and after (dashed histogram) the cut. About 40% of the events far from the $\eta \to \gamma\gamma$ peak are rejected. This reduces the $\pi^0\pi^0\eta_{miss}$ sample to $8,961$ events. The effect for $\pi^0\pi^0\eta'_{miss}$ results is very small. (table 1).

4.3 Remaining background

An event which is accepted as a $\pi^0\pi^0 P_{miss}$ final state (say $\pi^0\pi^0\pi^0_{miss}$) is rejected if it satisfies one of the other two final states (in this case $\pi^0\pi^0\eta_{miss}$ or $\pi^0\pi^0\eta'_{miss}$) with a $C.L. > 1\%$ ($\overline{fit}$ $\pi^0\pi^0 P_{miss}$ in table 1). This reduces the data sample by 15 to 20%.

[2] An asymmetric cut about the K_S mass was used because the K_S's were reconstructed as though their vertices were at the centre of the target.

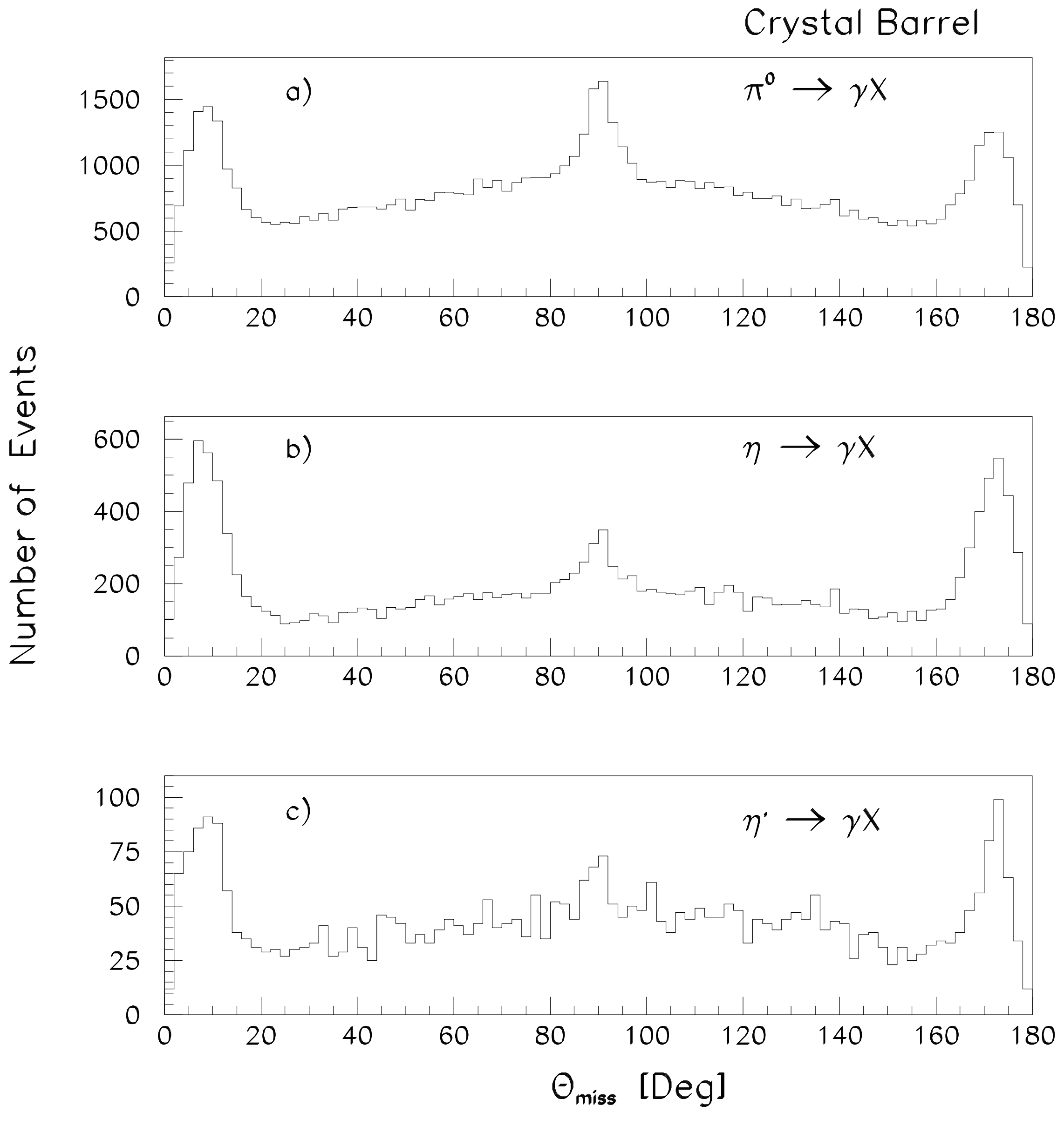

Figure 3: $\pi^0\pi^0P_{miss}$ *fit sample: Polar angular distribution of the missing photon in* $\pi^0\pi^0P_{miss}$ *events, P being a missing* π^0 *(a),* η *(b), or* η' *(c).*

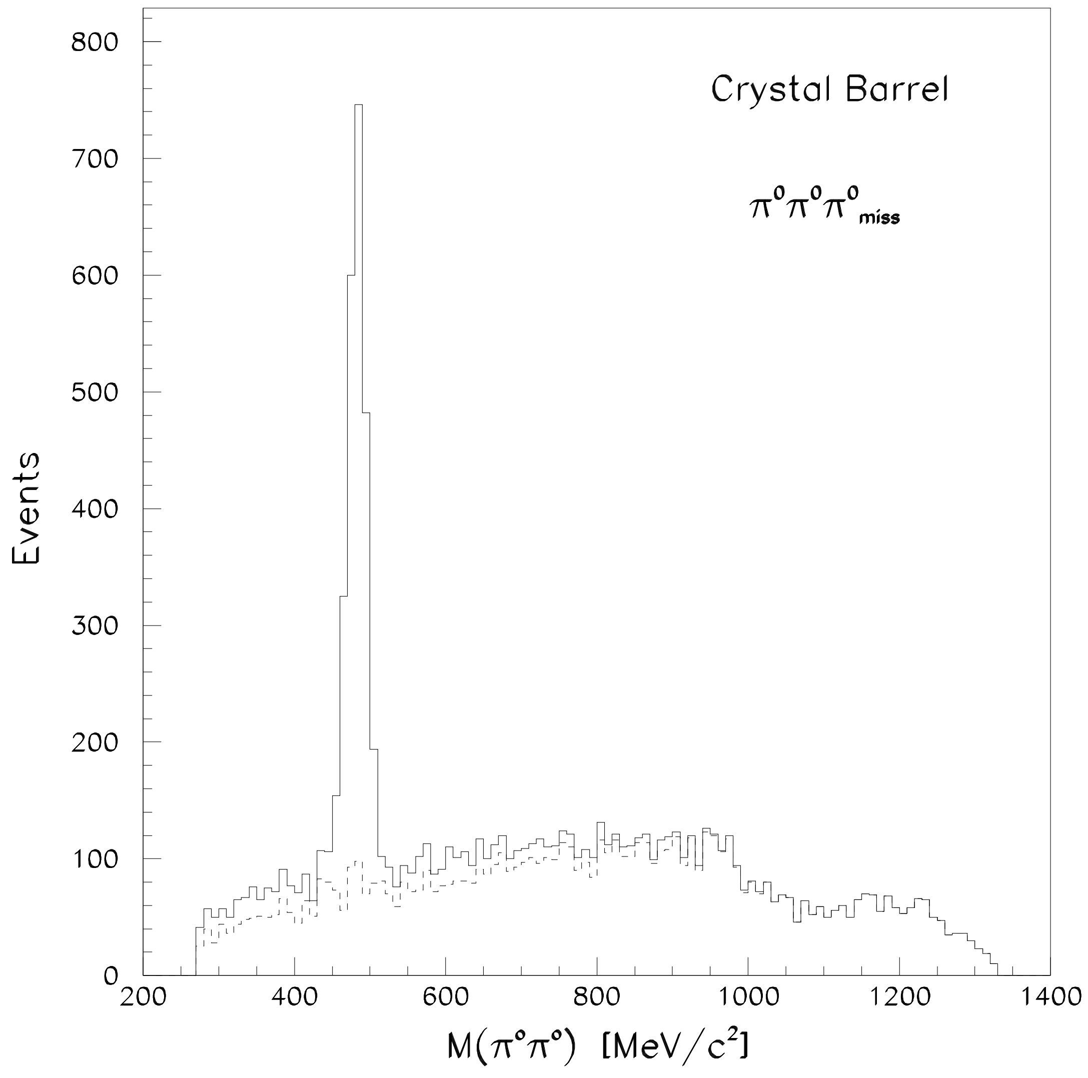

Figure 4: $\pi^0\pi^0\eta_{miss}$ *fit sample:* $\pi^0\pi^0$ *invariant mass before (full histogram) and after (dashed histogram)* $K_S K_L$ *rejection.*

The remaining background events tend to accumulate along the line of maximum possible γ energy in the laboratory, E_γ^{lab}, in a two dimensional plot E_γ^{lab} vs. E_γ^* (fig.5, see also MC studies in the next chapter). This happens for events where the fifth photon has

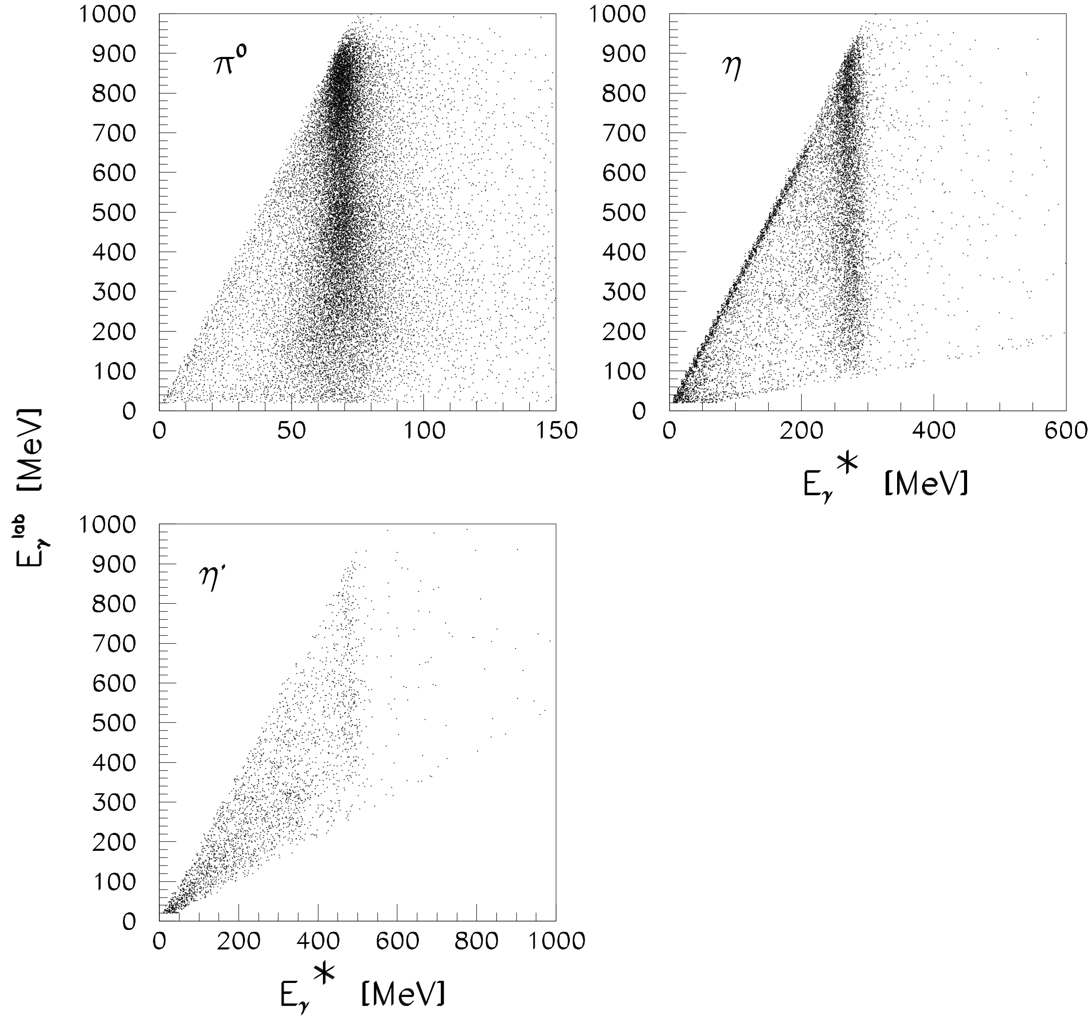

Figure 5: *Energy of the fifth γ in the laboratory (E_γ^{lab}) as a function of its energy in the P_{miss} rest frame (E_γ^*) before the $E_\gamma^{lab}/E_\gamma^*$ cut, P being a π^0, an η, or an η'.*

the same direction as P_{miss}. This is the case for the small fraction of $\pi^0\pi^0\gamma$ events (K_LK_S, $\omega\pi^0$, ...) that have not been removed by the above cuts. The following cuts are therefore applied: $E_\gamma^{lab}/E_\gamma^* \leq 11.0$ for π^0 decay, $E_\gamma^{lab}/E_\gamma^* \leq 2.8$ for η decay, and $E_\gamma^{lab}/E_\gamma^* \leq 1.6$ for η' decay. Up to 20% of the remaining background events are rejected by these cuts, without affecting the signal $P \to \gamma X$ (table 1), according to MC studies. The final sample consists of $24,503$ $\pi^0\pi^0\pi^0_{miss}$, $5,121$ $\pi^0\pi^0\eta_{miss}$ and $2,198$ $\pi^0\pi^0\eta'_{miss}$ events.

The photon energy E_γ^* in the P rest frame is shown for the 3 pseudoscalars before (fig.6) and after (fig.7) background reduction. Before discussing the Monte Carlo simulation it is interesting to try to distinguish the two categories of background events discussed at the beginning of this chapter, namely the events without and with missing energy and momentum. The energy distributions of the single photon in the π^0 rest are significantly different in both cases. This can be clearly seen if we plot E_γ^* for events:

- without missing energy and momentum (fig.8(a)). Before the kinematical fit the 5γ total momentum is required to be less than 100 MeV/c and the total energy to lie between 1700 and 1960 MeV. The remaining events, mainly $\omega\pi^0$ events, are kinematically fit to $\pi^0\pi^0\pi^0_{miss}$. The energy spread of the fifth photon $\sigma_{E_\gamma^*}$ is ~ 4.4 MeV.

- with missing energy and momentum ($E_{tot} \leq 1700$ MeV and $P_{tot} \geq 100$ MeV/c), mainly $3\pi^0$ (fig.8(b)). The distribution is much broader with $\sigma_{E_\gamma^*} \sim 10$ MeV.

This information will be used later, when fitting the data.

5 Monte Carlo Simulation

The next step is to check the method and determine the acceptance and energy resolution. A Monte Carlo program, based on the GEANT [18] package, which includes our detector geometry, is used to generate and simulate the various $\bar{p}p$ final states for both signal and background events. The simulated events are then passed through the same reconstruction and analysis chain as the real data. In the generation of signal events it is assumed that the particle X does not interact in the detector. Its mass is varied between 0 and m_P. As an example we discuss the the generated $\pi^0\pi^0\pi^0$ sample. One π^0 is forced to decay into γX. The photon energy E_γ^* in the π^0_{miss} rest frame is shown in fig.9 for $M_X = 100$ MeV/c^2 and $BR(\pi^0 \to \gamma X) = 10\%$. For $M_X \leq 65$ MeV/c^2 (corresponding to high γ energies) the missing photon background ($E_\gamma^* \sim m_{\pi^0}c^2/2$) is dominant. At higher mass range (smaller γ energy) the sensitivity is limited by the detection threshold for the photon (20 MeV in the laboratory frame). The detector is therefore most sensitive to M_X between ~ 65 and ~ 125 MeV/c^2 for π^0 decay. With the η and η' decays we can investigate higher X masses between ~ 50 and ~ 925 MeV/c^2.

The photon energy resolution varies between $\sigma = (4.0 - 5.0)$ MeV, $\sigma = (3.5 - 4.5)$ MeV, and $\sigma = (5.0 - 5.5)$ MeV, depending on M_X, for π^0, η and η' decay, respectively. On the $\pi^0 \to \gamma\gamma_{miss}$ peak the resolution is about 10 MeV. The lower and upper values correspond to the upper and lower limits, respectively, for M_X given above.

Important background sources were also simulated:

(i) $\bar{p}p \to \pi^0\omega$, ($\omega \to \pi^0\gamma$),

(ii) $\bar{p}p \to \pi^0\pi^0\pi^0$ ($\pi^0 \to \gamma\gamma$),

(iii) $\bar{p}p \to \pi^0\pi^0\eta$ ($\pi^0, \eta \to \gamma\gamma$), and

(iv) $\bar{p}p \to \pi^0\pi^0\eta'$ ($\pi^0, \eta' \to \gamma\gamma$).

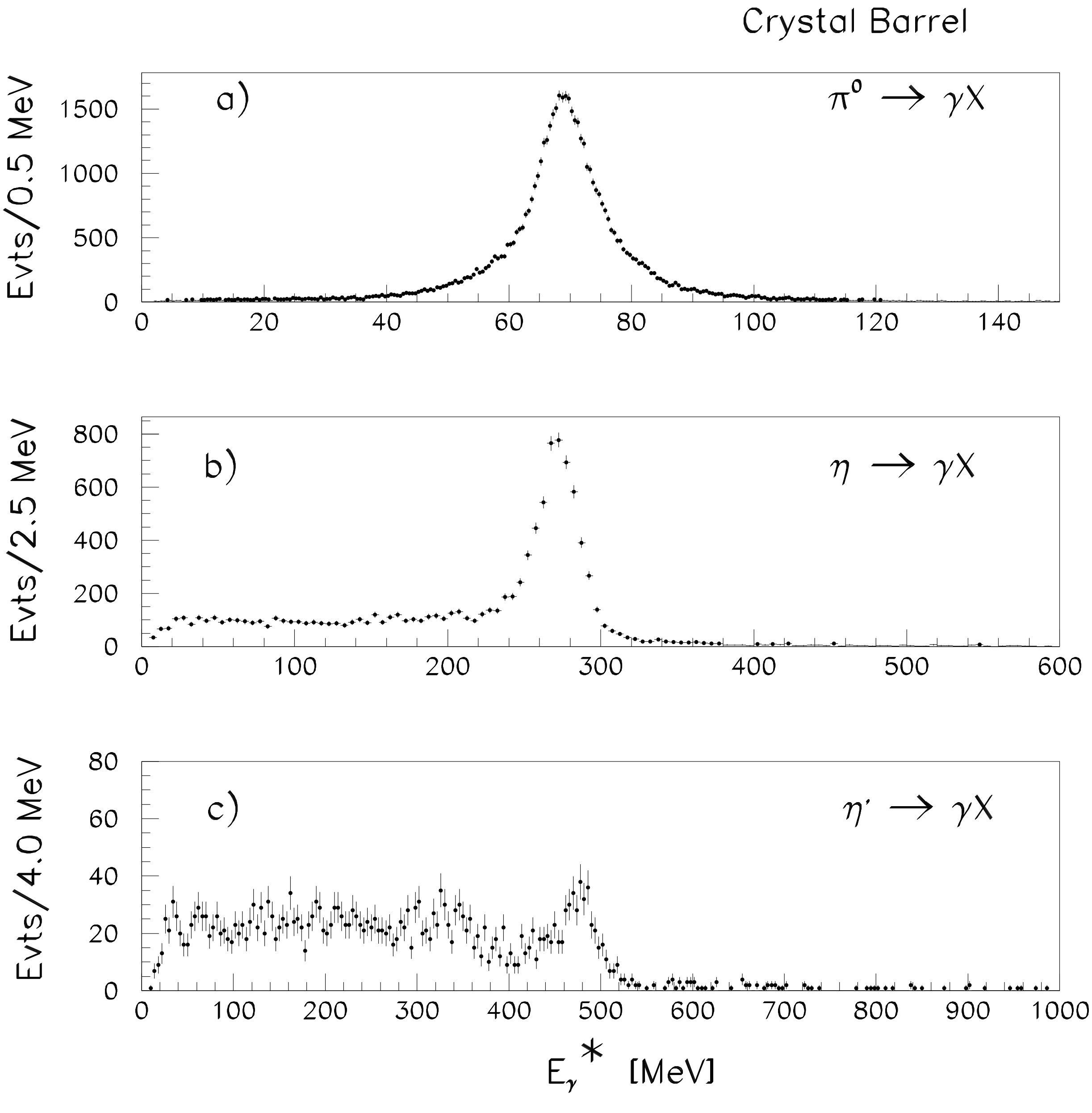

Figure 6: *Energy of the single γ in the P_{miss} rest frame for the $\pi^0\pi^0P_{miss}$ kinematically fit sample before background suppression, P_{miss} being a π^0 (a), an η (b), or an η' (c).*

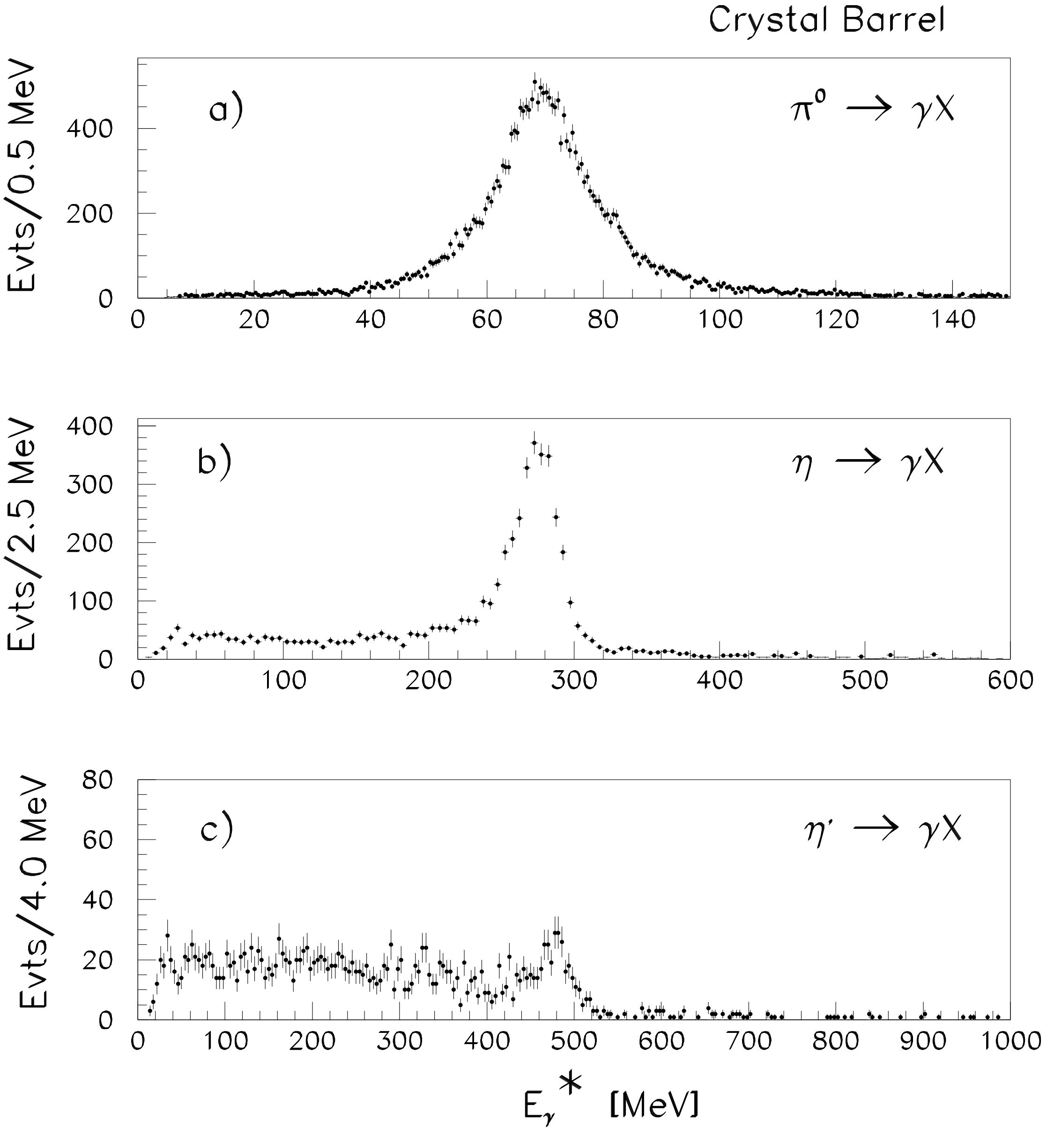

Figure 7: *Energy of the single γ in the P_{miss} rest frame for the $\pi^0\pi^0 P_{miss}$ kinematically fit sample after background suppression, P_{miss} being a π^0 (a), an η (b), or an η' (c).*

$\pi^0 \to \gamma X$

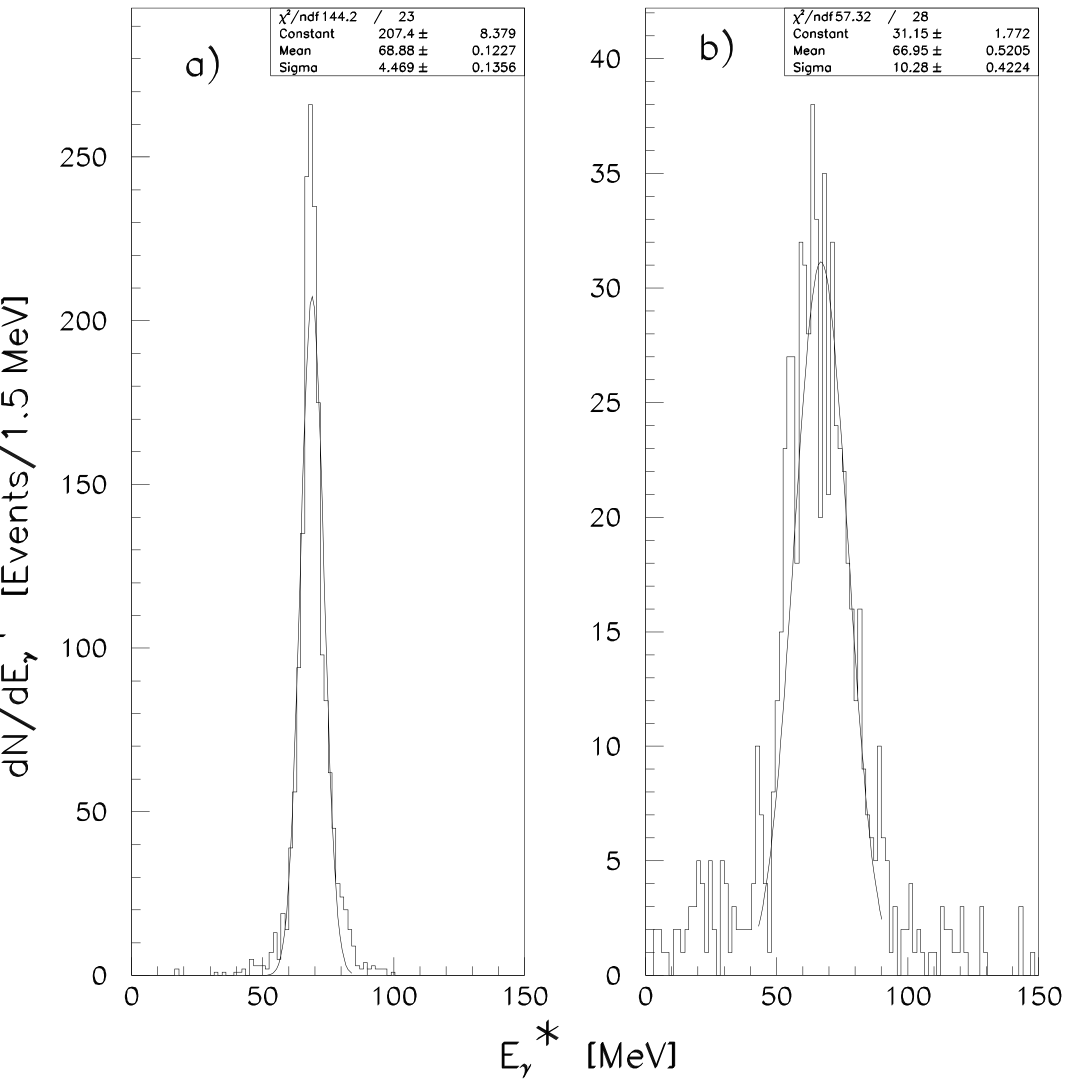

Figure 8: *Energy of the single γ in the π^0 rest frame for the $\pi^0\pi^0\pi^0_{miss}$ fit sample. Two samples are used: events without (a) and with (b) missing energy and momentum.*

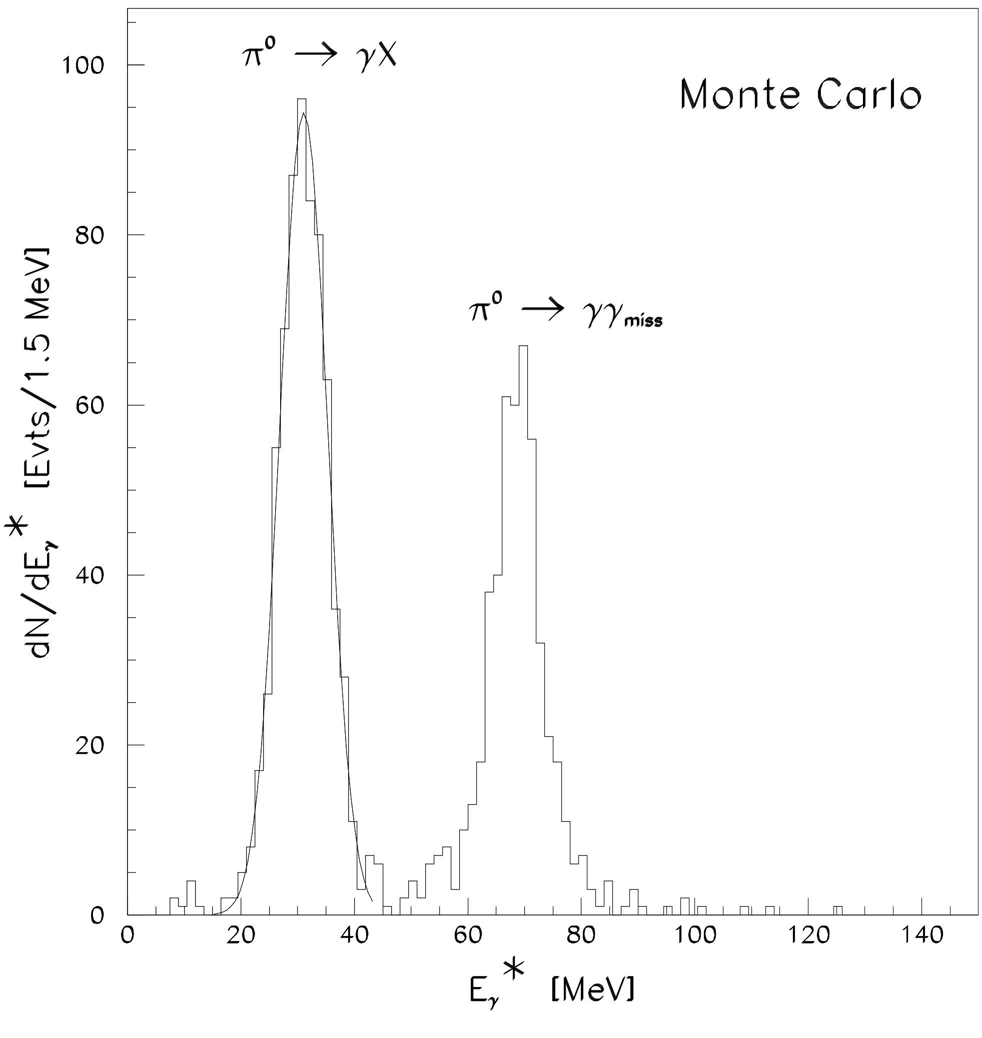

Figure 9: $\overline{p}p \rightarrow \pi^0\pi^0\pi^0$ *Monte Carlo simulated events, where* $BR(\pi^0 \rightarrow \gamma X) = 10\%$, $M_X = 100\ MeV/c^2$ *and* $BR(\pi^0 \rightarrow \gamma\gamma) = 90\%$. *Energy of the single* γ *in the* P_{miss} *rest frame for the* $\pi^0\pi^0 P_{miss}$ *kinematically fit sample.*

The signal events (with $P \rightarrow \gamma X$) are used to calculate the ratio of the number of accepted events to the number of generated events. The following efficiencies are obtained: $\epsilon_{\pi^0} = (11 \pm 1)\%$ for the π^0 decay, $\epsilon_\eta = (16 \pm 1)\%$ for the η decay, and $\epsilon_{\eta'} = (22 \pm 2)\%$ for the η' decay. The uncertainties include the dependence of the efficiency on M_X. The number of expected events for a given branching ratio $BR(X) = BR(P \rightarrow \gamma X)$ is

$$N_X = N_{\overline{p}} \times BR(\overline{p}p \rightarrow \pi^0\pi^0 P) \times BR(X) \times \epsilon. \tag{10}$$

For the $3\pi^0$ final state, a multiplicative factor 3 is included, to allow for the possible decay of any of the three π^0s. The 15×10^6 analysed 0-prong events correspond to $N_{\overline{p}} = (360 \pm 10) \times 10^6$ annihilations at rest. This has been determined by reconstructing annihilation events from $\overline{p}p \rightarrow \pi^0\pi^0$ and by using the absolute branching ratio $BR(\overline{p}p \rightarrow \pi^0\pi^0)$ [19]. We then expect $N_X^{\pi^0} = 76 \pm 11$, $N_X^{\eta} = 35 \pm 7$, and $N_X^{\eta'} = 38 \pm 7$ signal events for a branching ratio $BR(X)$ of 10^{-4}.

6 Results

6.1 $\pi^0 \rightarrow \gamma X$

The energy of the single γ in the π^0 rest frame is shown in fig.10. A ten-parameter fit to the data includes the sum of three gaussians and a constant background term. The three gaussians have maxima around $m_{\pi^0}c^2/2$ (at 69.2, 69.7 and 72.0 MeV). These peak positions and the widths (4.2, 10.3 and 26.0 MeV) are in agreement with what we expect for $\pi^0\omega$ events (no missing photon, 8(a)), $\pi^0\pi^0\pi^0$ events (where one photon is missing, 8(b)) and other smaller background sources. The third gaussian is, as expected, wider than the first two and its amplitude much smaller (32 events/0.5 MeV compared to 187 for the first and 263 for the second gaussian). It is due to channels like $\omega\pi^0\pi^0$ (where 2 photons are missing). The constant background term is due to events where the fifth photon found does not belong to the missing π^0. The global fit shows that the spectrum is well understood. The amplitudes are consistent with Monte Carlo predictions using the experimental branching ratios. We find that the 5γ final state $\pi^0\omega$ and the 6γ final state $\pi^0\pi^0\pi^0$ (where one photon from a π^0 is not reconstructed) together almost reproduce the shape of the π^0_{miss} data. The normalisation is given by the known branching ratios: $BR(\overline{p}p \rightarrow \pi^0\pi^0\pi^0) = (0.63 \pm 0.10)\%$, $BR(\overline{p}p \rightarrow \pi^0\omega) = (0.57 \pm 0.05)\%$ [19] and $BR(\omega \rightarrow \pi^0\gamma) = (8.5 \pm 0.5\%)$ [20] and the Monte Carlo reconstruction efficiencies. Other final states, like $\pi^0\eta\gamma$, $\eta\eta\gamma$, $\omega\pi^0\pi^0$ (where two photons are not reconstructed), and $\omega\omega$, $\omega \rightarrow \pi^0\gamma$ (where one photon is not reconstructed), give a smaller contribution.

To look for a signal various fits have been performed, with similar results:

- A gaussian with two free parameters (position and number of events) is fit to the data in the region between $E^*_\gamma = 10$ and 67.5 MeV. The width is fixed to the experimental resolution. The 10 parameters of the fit described above are allowed to vary within the errors.

- A signal (two parameters) and a polynomial background (three parameters) are fit to the data far from the $\pi^0 \rightarrow \gamma\gamma_{miss}$ peak.

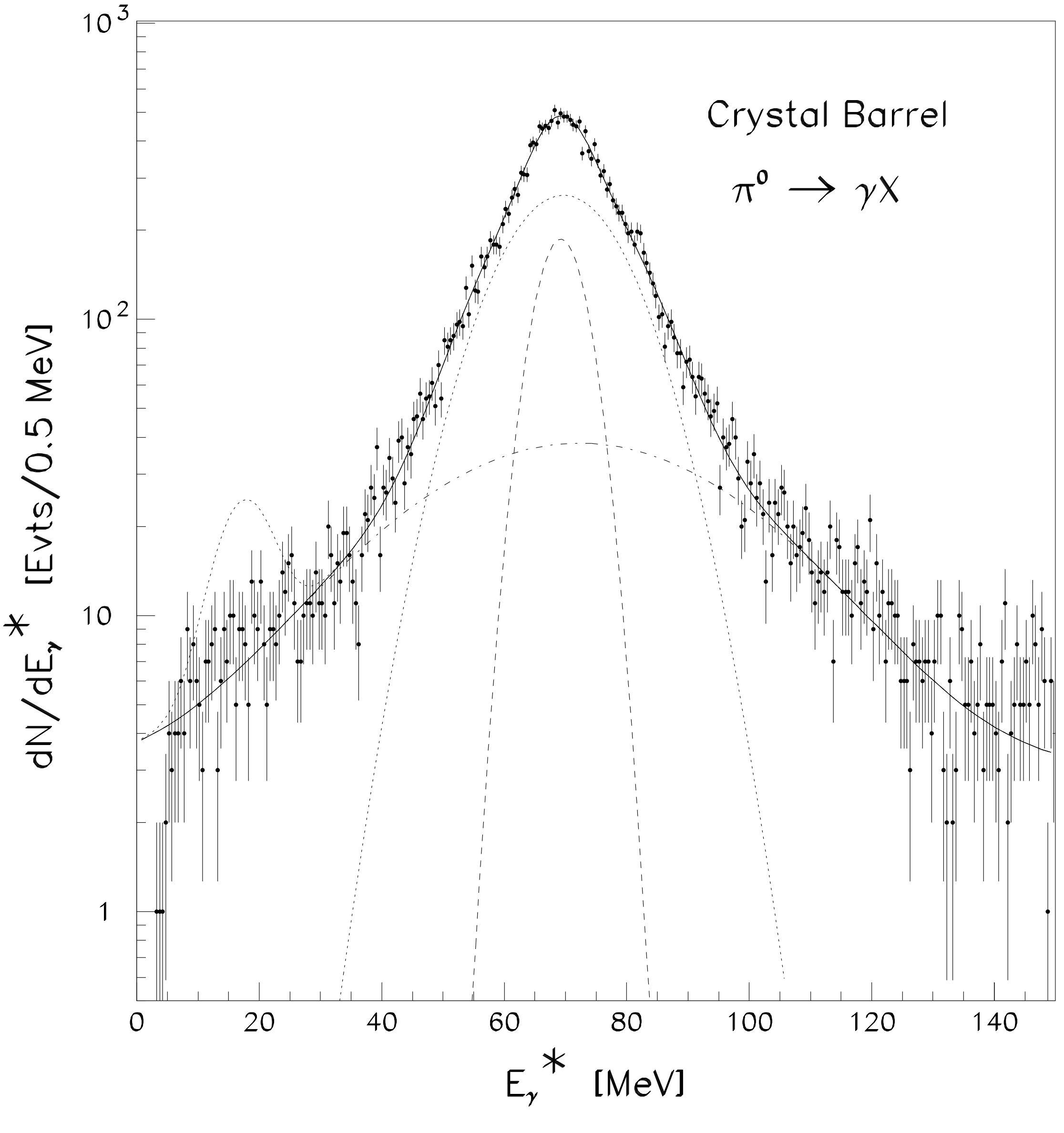

Figure 10: *Energy of the single γ in the π^0_{miss} rest frame for the $\pi^0\pi^0\pi^0_{miss}$ kinematically fit sample after background suppression, . The different contributions to the ten-parameter fit (full line) described in the text are shown separately: a narrow gaussian corresponding to $\pi^0\omega$ (dashed line), a broader gaussian corresponding to $\pi^0\pi^0\pi^0$, where one photon is missing (dotted line), a much broader gaussian corresponding to other final states (like $\pi^0\pi^0\omega$), where two photons are lost (dashed-dotted line) on top of a constant background. A signal corresponding to a branching ratio for $\pi^0 \rightarrow \gamma X$ with $M_X = 120$ MeV/c^2 of 5×10^{-4} is also drawn (dotted line).*

- A signal (two parameters), a polynomial background (three parameters), and two gaussians describing the $\pi^0 \rightarrow \gamma\gamma_{miss}$ peak (six parameters) are fit to the data between $E_\gamma^* = 10$ and 67.5 MeV.

An upper limit of $BR(\pi^0 \rightarrow \gamma X) < 6\times10^{-5}$ is obtained at 90% $C.L.$ for M_X lying between 65 MeV/c^2 and 125 MeV/c^2. Near $M_X = 0$ we obtain $BR(\pi^0 \rightarrow \gamma X) < 2.8 \times 10^{-4}$. A signal corresponding to $BR(\pi^0 \rightarrow \gamma X) = 5 \times 10^{-4}$ is also indicated in fig.10.

6.2 $\eta \rightarrow \gamma X$ and $\eta' \rightarrow \gamma X$

In the case of η and η' the photon energy distribution shows a flatter and lower background than in the π^0 case (fig.11 and 12, respectively). The main reason is the reduced contribution from 6γ events ($\pi^0\pi^0 P$, where one photon from the P is lost). This is due to the smaller BR for $\eta, \eta' \rightarrow \gamma\gamma$ (table 2), the higher γ efficiency for the η and η' decays and the lower combinatorial background (one for $\pi^0\pi^0\eta$ and $\pi^0\pi^0\eta'$ vs. three for $\pi^0\pi^0\pi^0$).

Pseudoscalar	Mass[MeV/c^2]	$BR(PS \rightarrow \gamma\gamma)$ [%]
π^0	134.98	98.80
η	547.45	38.8
η'	957.77	2.12

Table 2: *Branching ratio of π^0, η and η' into $\gamma\gamma$ [20].*

In fig.11 a six-parameter fit to the data is performed which includes one gaussian and a background term (second-order polynomial). No significant signal is found on top of the background curve. An upper limit of $BR(\eta \rightarrow \gamma X) < 6 \times 10^{-5}$ is obtained at 90% $C.L.$ for masses of the X boson between 200 MeV/c^2 and 525 MeV/c^2. A weaker upper limit of $BR(\eta \rightarrow \gamma X) < 3 \times 10^{-4}$ is obtained down to $M_X \sim 50$ MeV/c^2.

From fig.12 an upper limit of $BR(\eta' \rightarrow \gamma X) < 4 \times 10^{-5}$ is obtained at 90% $C.L.$ for masses of the X boson between 50 MeV/c^2 and 925 MeV/c^2. A signal corresponding to $BR(P \rightarrow \gamma X) = 5 \times 10^{-4}$ is indicated in fig.11 and 12 (dashed curves). The upper limit for the decay $P \rightarrow \gamma X$ as a function of E_γ^* and as as a function of mass is given in fig.13 for the three pseudoscalars.

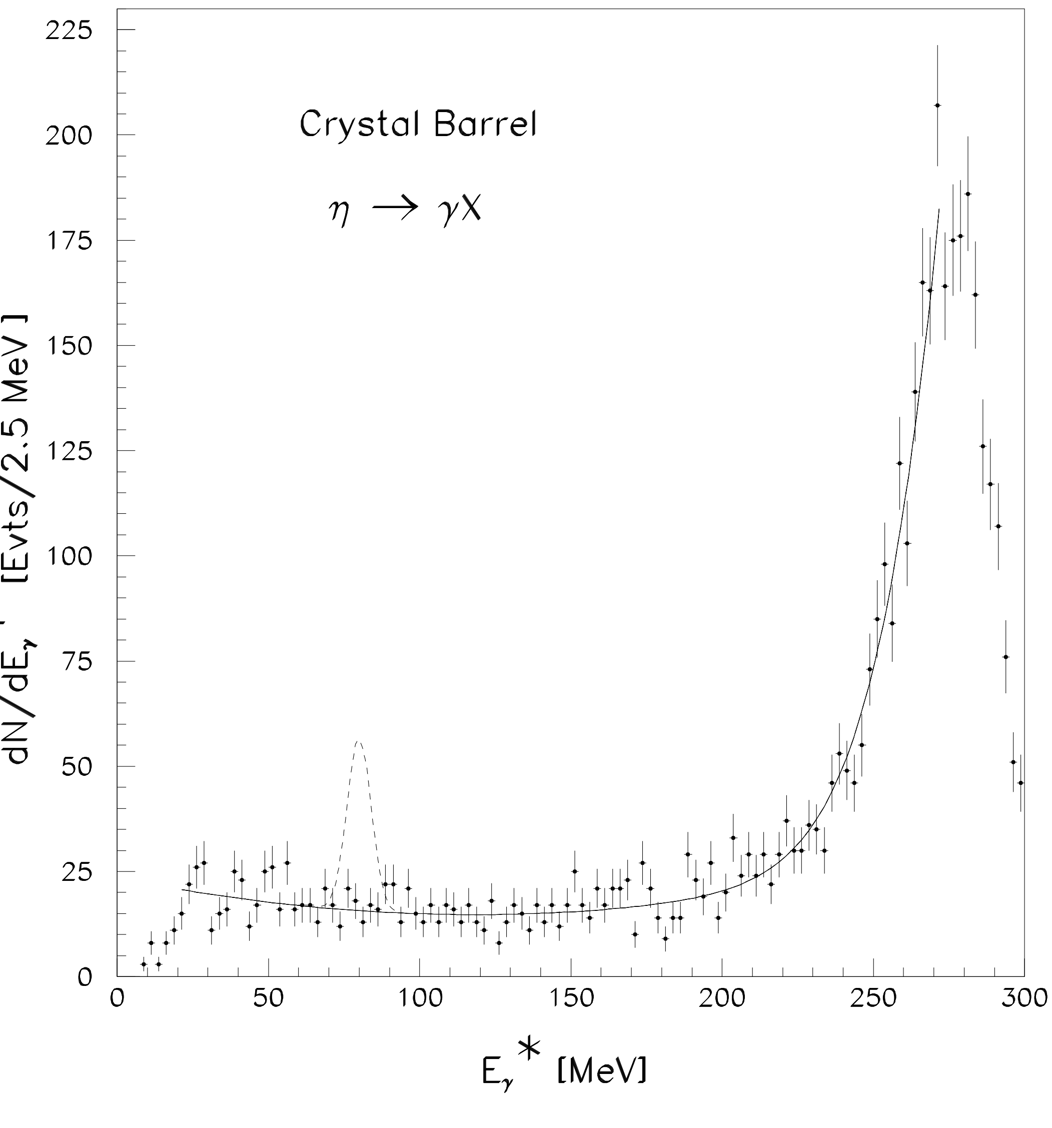

Figure 11: *Energy of the single γ in the η_{miss} rest frame for the $\pi^0\pi^0\eta_{miss}$ kinematically fit sample after background suppression. The full curve corresponds to a six-parameter fit to the data (gaussian + 2^{nd} order polynomial). A signal corresponding to a branching ratio of 5×10^{-4} for $\eta \rightarrow \gamma X$ with $M_X = 460$ MeV/c^2 of 5×10^{-4} is also indicated (dashed line).*

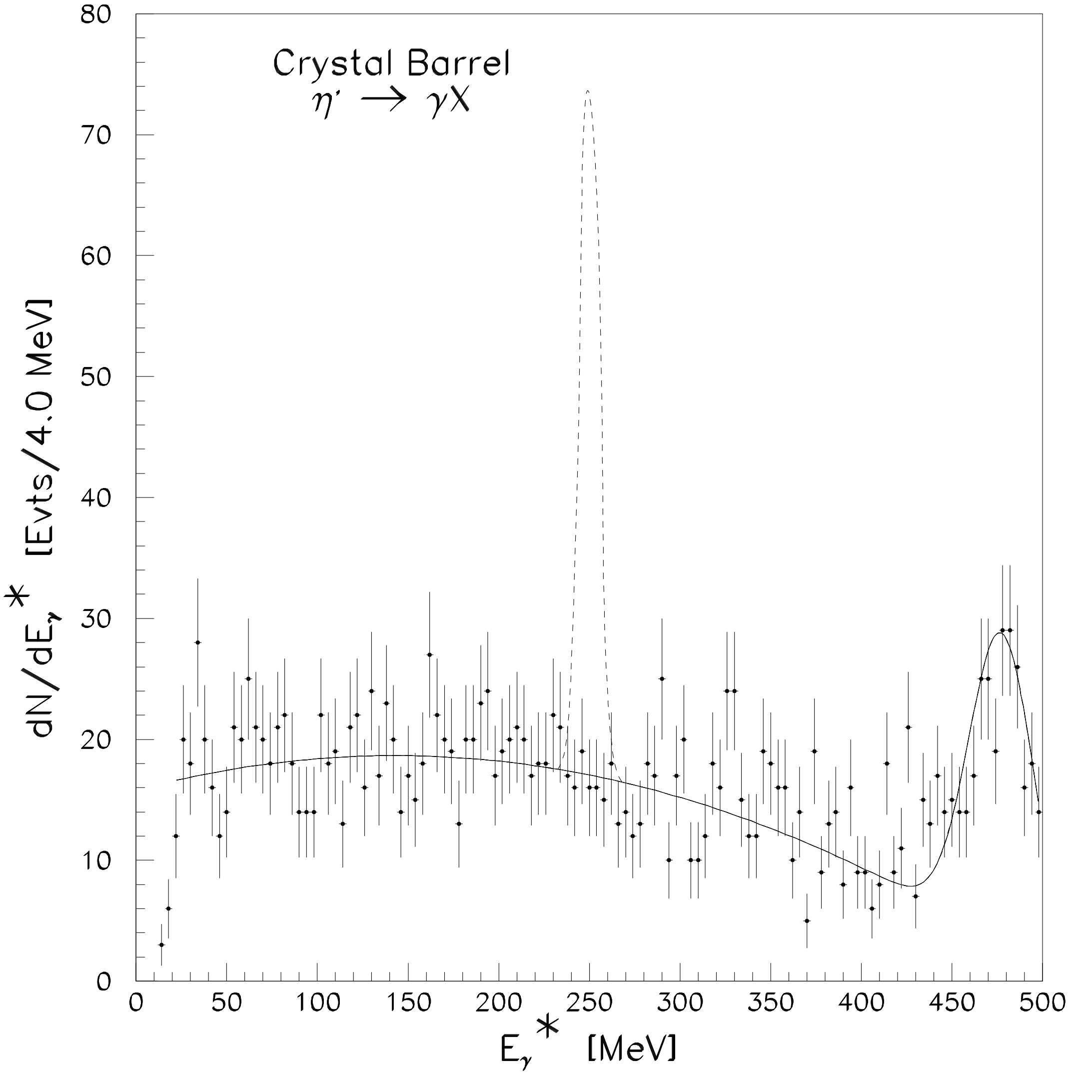

Figure 12: *Energy of the single γ in the η'_{miss} rest frame for the $\pi^0\pi^0\eta'_{miss}$ kinematically fit sample after background suppression. The full curve corresponds to a fit to the data (a gaussian around $m_{\eta'}/2$ and a 2^{nd} order polynomial elsewhere). A signal corresponding to a branching ratio of 5×10^{-4} for $\eta' \to \gamma X$ with $M_X = 662$ MeV/c^2 is also indicated (dashed line).*

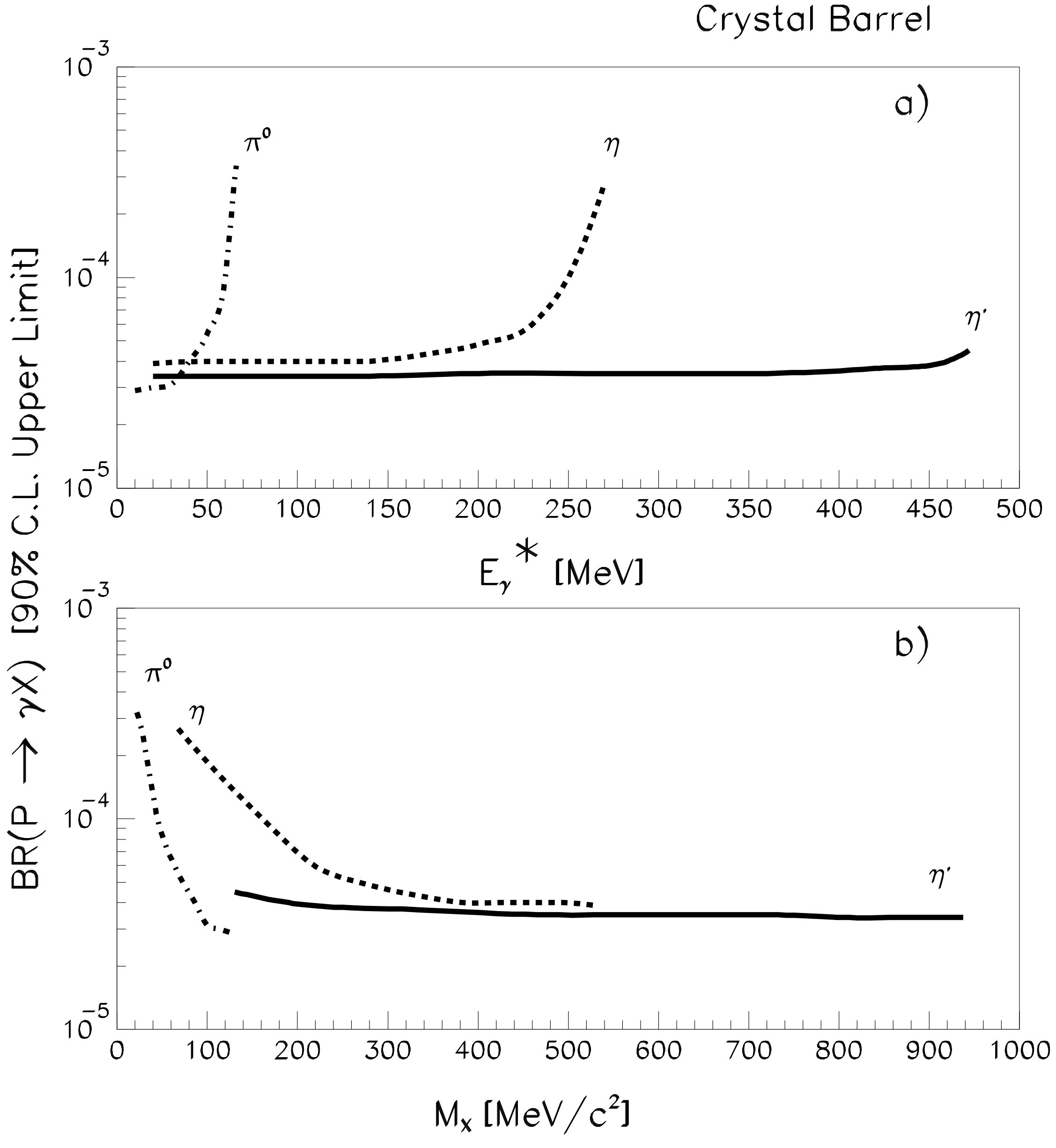

Figure 13: *Branching ratio upper limit (90% C.L.) for the decays $\pi^0 \rightarrow \gamma X$ (dashed-dotted line), $\eta \rightarrow \gamma X$ (dotted line) and $\eta' \rightarrow \gamma X$ (full line) as a function of E^*_γ (a) and as function of mass (b).*

7 Summary

Process	X decay	Experiment	BR upper limit	Comments
$\pi^0 \to \gamma X$	$X \to e^+e^-$	SINDRUM1[9]	4×10^{-6}	$10^{-23} < \tau_X < 10^{-11}$ sec
				$40 < M_X < 100$ MeV/c^2
	$X \to$ "anything"	BNL[11]	5×10^{-4}	$\tau_X > 10^{-7}$ sec
				$M_X < m_\pi$
	$X \to$ "anything"	TRIUMF[12]	$(2-7) \times 10^{-3}$	$\tau_X > 10^{-23}$ sec
				$25 < M_X < 100$ MeV/c^2
	$X \to$ "unseen"	CB[8][this work]	6×10^{-5}	$65 < M_X < 125$ MeV/c^2
			2.8×10^{-4}	$0 < M_X < 65$ MeV/c^2
$\eta \to \gamma X$	$X \to$ "unseen"	CB[8][this work]	6×10^{-5}	$200 < M_X < 525$ MeV/c^2
			3×10^{-4}	$50 < M_X < 200$ MeV/c^2
$\eta' \to \gamma X$	$X \to$ "unseen"	CB[this work]	4×10^{-5}	$50 < M_X < 925$ MeV/c^2

Table 3: *Directly measured upper limits for the decay of a pseudoscalar into a photon and a gauge boson X. $X \to$ "unseen" means X is not seen in the detector. $X \to$ "anything" includes the decay $X \to e^+e^-$.*

To summarise, we have searched for new light gauge bosons produced in π^0 and η decays by studying the kinematically well-constrained reactions $\overline{p}p \to \pi^0\pi^0 P$, where $P \equiv \pi^0, \eta, \eta'$ decays through the emission of a single photon recoiling against a missing state X (where X is a long-lived weakly interacting particle or $X \to \nu\overline{\nu}$). The method presented works and, in fact, can be used in other analyses. It can also be used to perform checks of the data. The different sources of background are well understood. We have analysed 15×10^6 "all-neutral" triggered events. No signal has been observed and branching ratio upper limits have been obtained. Our results, together with other direct measurements, are summarised in table 3. The π^0-decay limit improves the existing limit [11] by a factor of 4 to 8, whereas the η and η' upper limits have been measured for the first time, thereby extending the M_X range from 130 MeV up to 925 MeV. Our limits can be applied to any weakly interacting vector boson.

8 Acknowledgement

We would like to thank the technical staff of the LEAR machine group and of all the participating institutions for their invaluable contributions to the success of the experiment. We acknowledge financial support from the German Bundesministerium für Forschung und Technologie, the Schweizerischer Nationalfonds, the British Particle Physics and Astronomy Research Council and the U.S. Department of Energy (contract No. DE-FG03-87ER40323, DE-AC03-76SF00098, and DE-FG02-87ER40315). F.-H. Heinsius and K.M. Crowe acknowledge support from the A. von Humboldt Foundation. We thank Dr. S. Gninenko who first brought this research subject to our attention.

References

[1] P. Langacker, *Phys. Rep.* **72C**(1981)185.

[2] P. Fayet, *Phys. Lett.* **69B**(1977)489; *Nucl. Phys.* **B187**(1981)184; S. Weinberg, *Phys. Rev.* **D26**(1982)287.

[3] J. Ellis et al., *Nucl. Phys.* **B276**(1986)14; J. Schwarz, *Superstrings: the First 15 Years*, World Sc. Pub., Singapore (1985).

[4] S. L. Glashow, *Proc. Conf. Rencontres de Moriond*, (1986).

[5] F. Cuypers and P.H. Frampton, *Phys. Rev. Lett.* **60**(1988)1237; J. Bagger, C. Schmidt and S. King, *Phys. Rev.* **D37**(1988)1188; P.H. Frampton and S.L. Glashow, *Phys. Lett.* **B190**(1987)157.

[6] M.I. Dobroliubov and A.Yu. Ignatiev, *Nucl. Phys.* **B309**(1988)655.

[7] M.I. Dobroliubov, *Yad. Fiz.* **52**(1990)551. [*Sov. J. Nucl. Phys.* **52**(1990)352].

[8] C. Amsler et al., *Phys. Lett.* **B333**(1994)271.

[9] R. Meijer Drees et al., Phys. Rev. Lett. **68**(1992)3845.

[10] C.M. Hoffman, *Phys. Lett.* **B208**(1988)149.

[11] M. S. Atiya et al., *Phys. Rev. Lett.* **69**(1992)733.

[12] R. Meijer Drees et al., Phys. Rev. **D49**(1994)4937.

[13] F. Ould-Saada (Crystal Barrel Collab.), HEP Conf., Glasgow (1994); LEAP Conf., Bled (1994).

[14] C. Amsler et al., *Phys. Lett.* **B342**(1995)433.

[15] C. Amsler et al., *Phys. Lett.* **B322**(1994)431.

[16] Crystal Barrel, unpublished preliminary result.

[17] E. Aker et al., *Nucl. Instrum. Methods* **A321**(1992)69.

[18] R. Brun et al., Internal Report CERN DD/EE/84-1, CERN 1987.

[19] C. Amsler et al., *Z. Phys.* **C58**(1993)175.

[20] Review of Particle Properties, *Phys. Rev.* **D50**(1994)1173.